

Supporting Information

Template-Stabilized Oxidic Nickel Oxygen Evolution Catalysts

Nancy Li,^a Thomas P. Keane,^a Samuel S. Veroneau,^a Ryan G. Hadt,^{b,c} Dugan Hayes,^{b,d} Lin X. Chen,^{b,e} and Daniel G. Nocera^{*,a}

^a *Department of Chemistry and Chemical Biology, Harvard University, Cambridge, MA 02138*

^b *Chemical Sciences and Engineering Division, Argonne National Laboratory, Lemont, IL 60439*

^c *Division of Chemistry and Chemical Engineering, California Institute of Technology, Pasadena, CA 91125*

^d *Department of Chemistry, University of Rhode Island, Kingston, RI 02881*

^e *Department of Chemistry, Northwestern University, Evanston, IL 60208*

dnocera@fas.harvard.edu

Table of Contents

<i>Index</i>	<i>Page</i>
Experimental Methods	S3
Figure S1. Cyclic voltammograms of PbNiO _x and PbNiFeO _x deposition	S7
Table S1. Elemental composition of PbO _x -based films	S8
Figure S2. SEM images of PbO _x -based films	S9
Figure S3. SEM/EDS elemental maps of PbO _x -based films	S10
Figure S4. Summary of PbO _x and NiO _x films stability and V _{1mA} in acid	S11
Figure S5. Faradaic efficiency of O ₂ evolution from PbNiFeO _x	S12
Figure S6. Tafel plots of PbNiFeO _x in in B _i and P _i solutions	S13
Figure S7. Tafel plots and V _{1mA} for PbNiFeO _x films with varying Ni:Fe content	S14
Figure S8. XPS Ni 2p of PbNiO _x and PbNiFeO _x films	S15
Figure S9. XAS Ni K-edge spectrum of PbNiO _x and PbNiFeO _x films under OER	S16
Figure S10. XPS Pb, O, and Ni spectra of PbCoFeO _x films under OER over time	S17
Figure S11. ICP-MS composition of PbO _x based films after OER	S18
Figure S12. SEM images of PbNiFeO _x film surface throughout OER in acid	S19
Figure S13. Cyclic voltammograms of mixed-metal films in acidic conditions	S20
Figure S14. Structures of α-PbO ₂ and β-PbO ₂	S21
References	S22

Experimental Methods

Materials. Ni(NO₃)₂•6H₂O (99.999%) was used as received from Strem. Pb(NO₃)₂ (99.999%), (NH₄)₂Fe(SO₄)₂•6H₂O (99.997%), H₃PO₄ (99.999%), and H₂SO₄ (99.999%) were used as received from Sigma Aldrich. KNO₃ (99.9%) was used as received from Macron. KOH (<0.001% Ni, Fe, and other heavy metals) was used as received from EMD Millipore. TraceSELECT Ultra nitric acid and TraceSELECT standards for ICP were used as received from Fluka Analytical. Methylphosphonate, CH₃P(O)(OH)₂ (MeP_i), was purchased from Sigma Aldrich and then recrystallized twice from acetonitrile (HPLC grade, Sigma Aldrich). All electrolyte solutions were prepared with type I water (EMD Millipore, 18.2 MΩ cm resistivity). Fluorine-doped tin-oxide coated glass (FTO; TEC-7) was purchased as pre-cut 1 cm × 2.5 cm glass pieces from Hartford Glass with 7 Ω/sq surface resistivity.

General Electrochemical Methods. All electrochemical experiments were conducted on a CH Instruments 760D bipotentiostat, using an Ag/AgCl reference electrode (BASi, filled with saturated KCl), and a Pt-mesh (99.9% Alfa Aesar) counter electrode in a three-electrode electrochemical cell with a porous glass frit separating the working and auxiliary compartments.

All glassware was acid cleaned by soaking in aqua regia followed by copious rinsing with type I water (EMD Milipore, 18.2 MΩ cm resistivity). Prior to use, FTO slides were cleaned by sonication in acetone and then rinsed with type I water. A 1 cm² geometric electrode area was created by masking the FTO with Scotch tape. An Ag/AgCl reference electrode was positioned close to the FTO in the working compartment, and a Pt mesh electrode in the auxiliary side of the H-cell was used to complete the circuit.

Electrode potentials were converted to the NHE scale using $E(\text{NHE}) = E(\text{Ag}/\text{AgCl}) + 0.197 \text{ V}$. Overpotentials for the oxygen evolution reaction from water were computed using $\eta = E(\text{NHE}) - (1.23 \text{ V} - 0.059 \text{ V} \times \text{pH})$. All measurements were performed at room temperature (23 ± 1 °C).

Electrodeposition of Films. As-deposited films were prepared by applying a constant anodic potential to 1 cm² FTO for a specified amount of time in a 50 mM MeP_i solution buffered at pH 8.0 containing a total of 0.5 mM metal solution. Electrodeposition conditions are based on previously published methods:¹ NiFePbO_x at 1.3 V for 1 h from solutions of 0.25 mM Fe²⁺, 0.125 mM Ni²⁺, and 0.125 mM Pb²⁺; NiPbO_x at 1.3 V for 40 min from 0.25 mM Ni²⁺ and 0.25 mM Pb²⁺; FePbO_x at 1.2 V for 1.5 h from solutions of 0.25 mM Fe²⁺ and 0.25 mM Pb²⁺; PbO_x at 1.35 V for 40 min from solutions of 0.5 mM Pb²⁺. To minimize precipitation of metal hydroxides from these solutions, 25 mL of 0.1 M MeP_i was added to 25 mL of 1 mM total metal solution. All deposition protocols aimed to achieve roughly similar mass loading of films. After deposition, films were briefly immersed in type I water to remove any lingering metal ions and subsequent electrochemical characterization was performed immediately unless otherwise noted.

Scanning Electron Microscope (SEM). After completion of film deposition, the electrodes were gently rinsed in type I water and immersed in 0.1 M KP_i + 1 M KNO₃ pH 2.5 buffer.

Films were held at a constant current of 1 mA cm^{-2} while stirring at 400 rpm for 10 min unless otherwise noted and then rinsed in type I water. Excess water was then wiped off the back of the film and catalyst films were air-dried overnight. Field emission scanning electron microscopy (FESEM) was performed with a Zeiss Supra55VP. The FESEM was operated at a beam voltage of 15 kV at a working distance of 8.5 mm with a $20 \text{ }\mu\text{m}$ aperture and a secondary electron (SE2) detector. Elemental quantification was determined at a beam voltage of 13 kV with an energy dispersive X-ray spectrometer using EDAX ZAF correction factors. Homogeneity of films were evaluated by EDS elemental maps using characteristic X-rays at the K-edge for Ni, Fe, and O, L-edge for Sn, and M-edge for Pb. Scans were taken at 512×400 pixel resolution and averaged over 16 frames.

Acid Stability During Oxygen Evolution. The stability of catalyst films for oxygen evolution in acid buffers was assessed by long-term chronopotentiometry. Unless otherwise noted, $0.1 \text{ M KPi} + 1.75 \text{ M KNO}_3$ at pH 2.5 was used as the buffer. A 50 mL, two compartment H-cell was used, and the electrolyte was stirred at 400 rpm in the working and reference electrode compartment to decrease local pH gradients during prolonged electrolysis. Chronopotentiometry was performed on freshly prepared catalyst films (after a quick gentle rinsed in type I water) at 1 mA cm^{-2} and the potential was recorded over time until film dissolution was noted by a sudden jump in potential to 2.7 V (potential required for 1 mA cm^{-2} of OER by blank FTO). Independently prepared films were made and tested for acid stability three times to ensure reproducibility.

Tafel Slope Collection. The oxygen evolution activities of freshly prepared catalyst films were determined by measuring the steady-state current density (j) as a function of applied potential (E) in solutions of $100 \text{ mM KPi} + 1 \text{ M KNO}_3$ at pH 2.5. Steady state conditions were obtained by holding the films at each discrete potential for 100 s to allow for the current to converge. The measurements were initiated at the highest potential first to further minimize any pseudocapacitance. Solutions were stirred at 400 rpm with a Teflon stir bar (sufficient to remove mass transport limitations) and the applied potentials were post corrected for uncompensated resistance by subtracting iR (measured on a blank FTO in the same solution conditions). Typical values of uncompensated resistance are $\sim 17 \text{ }\Omega$. Further precautions were exercised by targeting Tafel data collection at current densities between $1 \text{ }\mu\text{A}$ and 1 mA cm^{-2} . The current-potential data were plotted as $\log j$ vs. overpotential (η) to construct Tafel plots. The measured intercept and slope from independently prepared films under the same conditions were reproduced three times.

Cyclic Voltammetry (CV). Blank FTO was transferred to the deposition solution containing Pb, Ni, and/or Fe salts. CV scans were initiated at 0 V and then scanned towards positive potentials until $\sim 2 \text{ mA}$ of current was obtained at which point the polarity of the scan was reversed towards negative potentials until -0.8 V when the polarity was switched again ultimately ending at 0 V. Scans were run without pause in quiescent solution at a scan rate of 0.1 V/sec with iR compensation corrected through automatic positive feedback.

Faradaic Efficiency of Oxygen Evolution. The faradaic efficiency of oxygen evolution on NiFePbO_x films was determined in $0.1 \text{ M KPi} + 1 \text{ M KNO}_3$ at pH 2.5 using a gas

chromatograph as previously published.¹ The film was mounted into a custom-built two-compartment electrochemical cell where a cation-exchange membrane (Nafion 117, Sigma Aldrich) was used to separate the two chambers. An Ag/AgCl-based leak-free reference electrode (LF-1, Warner Instruments) was used as the reference electrode and a Pt wire was the counter electrode. A Viton O-ring was applied to define the area of working electrode and OER was sustained at constant current density of 1 mA cm⁻². While stirring, a constant flow of Ar gas (20 sccm) was bubbled through the chamber containing the working/reference electrodes. The gas outlet was connected to a gas chromatograph equipped with a thermal conductivity detector (multiple gas analyzer #3, SRI Instruments). The amount of O₂ in the out-fluxing Ar gas was quantified based on the calibration with known O₂ concentrations. Initial control experiments were performed to ensure that O₂ in the air has no contribution to the measured O₂ signals. The detected O₂ concentrations were compared to the theoretical yield of O₂, which was calculated by dividing the charge passed by 4 Faraday to obtain the faradaic efficiency.

X-Ray Absorption Spectroscopy. *In situ* Pb L₃-edge and Ni K-edge X-ray absorption near-edge spectra (XANES) were recorded on catalyst films prepared by electrodeposition on an X-ray transparent indium tin oxide coated poly(ethylene terephthalate) sheet (ITO-PET) with resistance of 60 Ω/sq and ITO coating of 1300 Å thickness (Sigma Aldrich). The ITO-PET sheets were fit to a home-made Teflon cell for XAS experiments. A 3 cm × 5 cm sheet of ITO was covered with tape to expose 1 cm × 1 cm for deposition and 5 mm at the top for connection to the potentiostat. Unless otherwise noted, catalyst films were held at 1.9 V in 0.1 M KP_i + 1 M KNO₃ pH 2.5 and stirred at 400 rpm.

Ni K-edge and Pb L₃-edge XANES spectra were collected at beamline 12 BM at the Advanced Photon Source at Argonne National Laboratory using a Si(111) X-ray monochromator with a focused beam size of ~0.5 × 0.5 mm. All data were collected in fluorescence mode using a 13-element Ge Canberra detector. Energy calibration was carried out using Ni foil and Pb foil. XAS data were collected at room temperature using a home-made *in situ* XAS cell. No sample damage due to X-ray beam exposure was observed after multiple scans using the same sample/electrode position. Three to five scans were averaged for analysis. Background subtraction and data normalization were carried out using the Athena software package.²

X-Ray Photoelectron Spectroscopy (XPS). After completion of film deposition, the electrodes were gently rinsed in 18 MΩ distilled water and immersed in 0.1 M KP_i + 1 M KNO₃ pH 2.5. Films were held at a constant current of 1 mA cm⁻² for 10 min with stirring at 400 rpm unless otherwise noted and then rinsed in type I water. PbO_x and FePbO_x films were held at 2.0 V (as opposed to the high potential of 2.7 V necessary to achieve 1 mA cm⁻² of OER in these film) to be more reflective of the potentials held by NiPbO_x-based films. Excess water was then wiped off the back of the film and catalyst films were air-dried overnight. All samples were illuminated using a monochromated Al Kα X-ray source (1486.6 eV energy and 0.85 eV line width)³ with a 400 μm spot size. Surface charging was compensated by a low energy (0–14 eV) electron flood gun. The system was pre-calibrated with Au, Ag, and Cu standards built into the sample stage using an automated routine. High-resolution

spectra for Ni 2p, Pb 4f, C 1s, and O 1s were measured with a step size of 0.1 eV. Spectra for Ni and O were averaged from 50 scans, Pb from 30 scans, and C from 20 scans. All spectra were then calibrated to the C 1s peak at 284.8 eV and normalized.⁴

Inductively Coupled Plasma Mass Spectrometry (ICP-MS). Trace elemental analysis was carried out with quadrupole ICP-MS (Thermo Electron, X-Series ICP-MS with collision cell technology). All pipettes and polypropylene tubes were soaked in ~5% TraceSELECT nitric acid overnight and rinsed with type I water. All pipette tips were pre-rinsed with 2% double-distilled trace nitric acid prior to use. Films were digested by soaking in 20% double distilled trace nitric acid over two days. FTO substrates were then scanned by cyclic voltammetry after soaking in 20% nitric acid to ensure complete film digestion. ICP samples were diluted to 2% nitric acid prior to analysis. Film samples along with standards and controls were then scanned twice for 60 s each for ⁵⁶Fe, ⁶⁰Ni, and ²⁰⁸Pb. Internal standards and controls dispersed throughout the samples were run to confirm no signal drift.

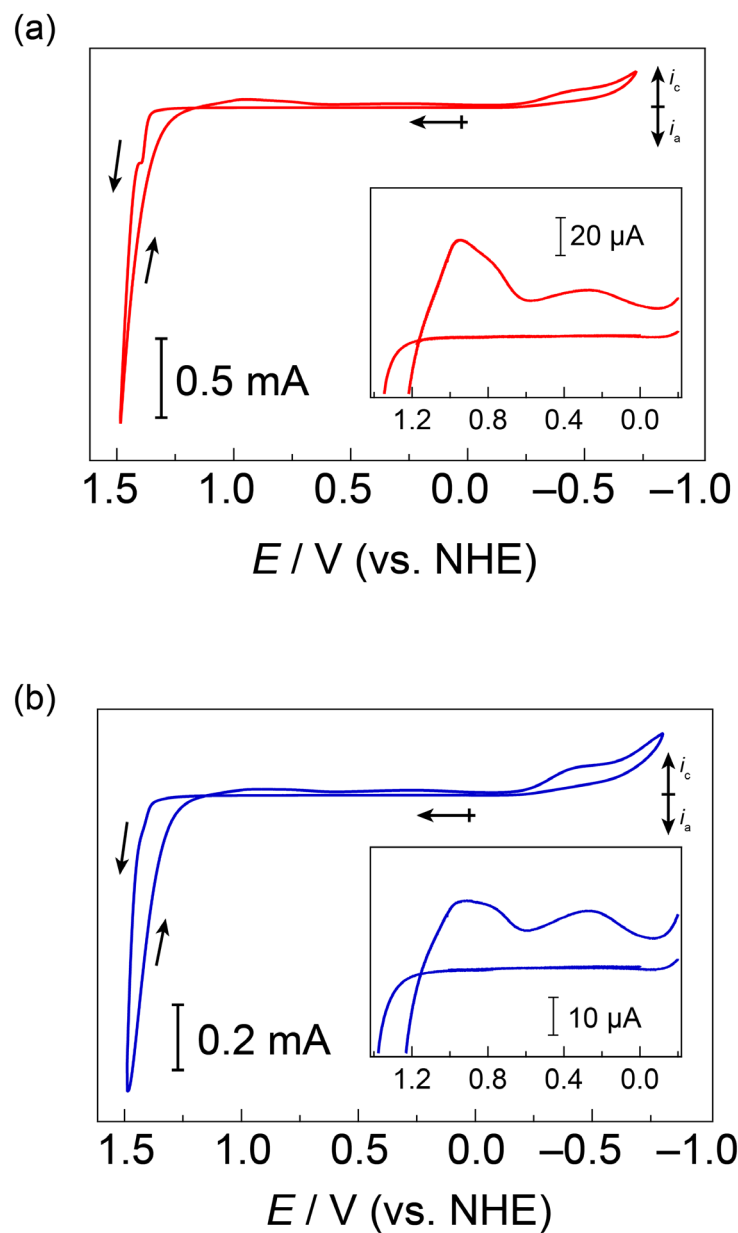


Figure S1. Cyclic voltammograms (CVs) of a 1 cm² FTO electrode in 50 mM MePi buffer at pH 8.0 with 0.25 mM total metal concentration: (a) Ni²⁺ and Pb²⁺ (red —), and (b) Fe²⁺, Ni²⁺, and Pb²⁺ (blue —). Scan rate is 100 mV s⁻¹.

Table S1. Elemental composition of PbO_x based films as-deposited and after operating OER at 1 mA cm⁻² in 0.1 M KP_i + 1M KNO₃ pH 2.5 for 40 h.

Film	Condition	Total metal mol	Pb mol %	Ni mol %	Fe mol %
NiPbO _x	as-deposited	277.3 ± 6.9	49.7 ± 1.2	50.3 ± 0.3	-
	40 h OER in 0.1 M KP _i + 1.75 M KNO ₃ pH 2.5	63.4 ± 6.3	97.2 ± 0.9	2.8 ± 0.7	-
NiFePbO _x	as-deposited	255.7 ± 11.2	39.0 ± 0.8	30.1 ± 0.6	30.9 ± 1.2
	40 h OER in 0.1 M KP _i + 1.75 M KNO ₃ pH 2.5	89.3 ± 15.3	85.9 ± 2.6	3.8 ± 2.3	10.3 ± 2.3

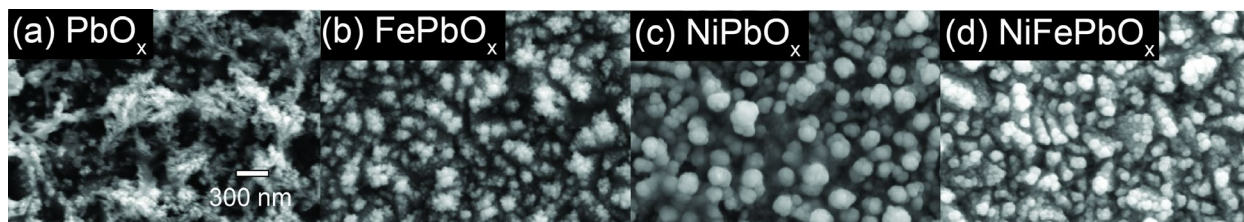


Figure S2. SEM images of (a) PbO_x, (b) FePbO_x, (c) NiPbO_x, and (d) NiFePbO_x for comparison. All samples were prepared on FTO substrate, and scale bar indicates 300 nm.

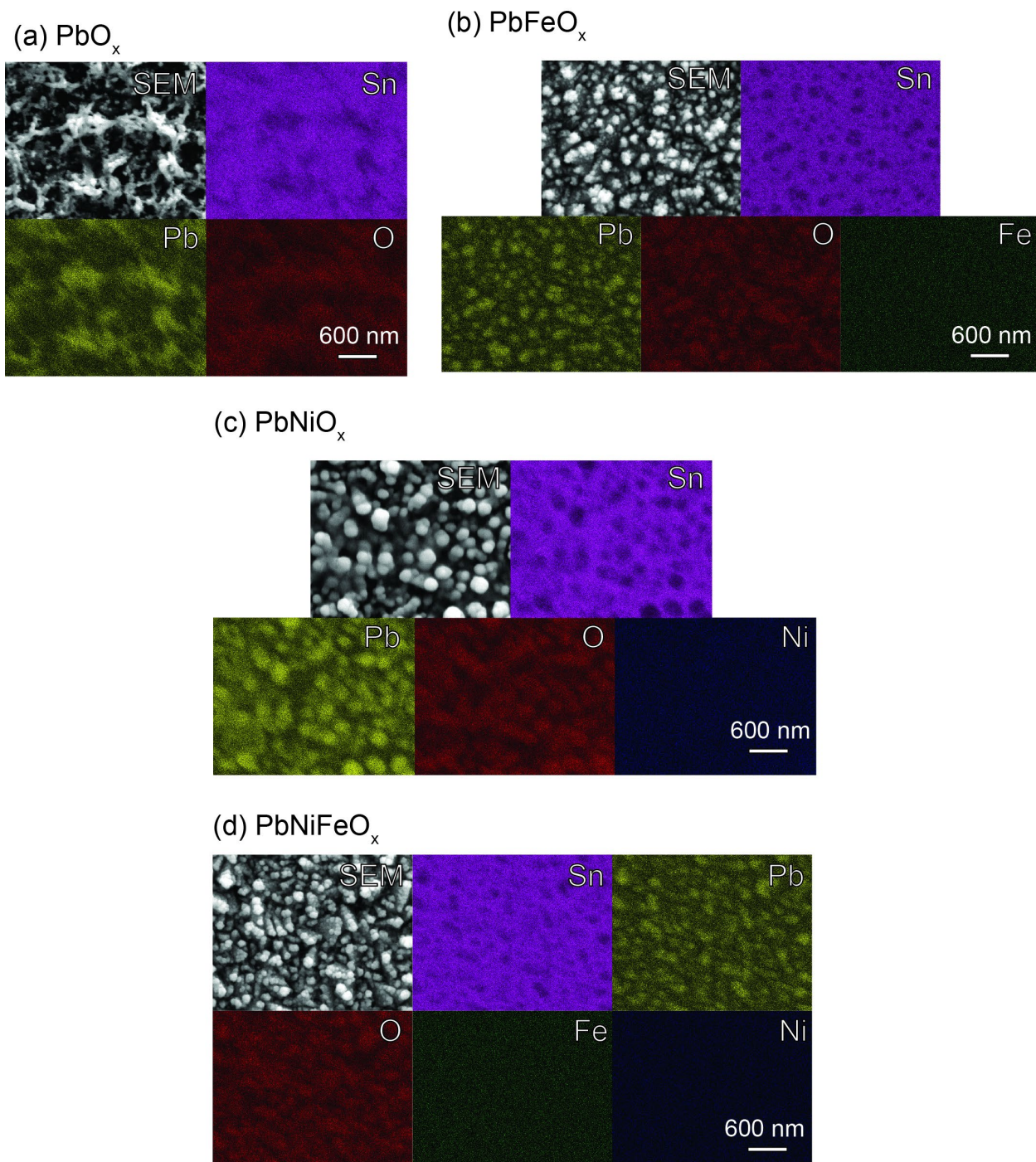


Figure S3. EDS elemental maps recorded through SEM of (a) PbO_x , (b) FePbO_x , (c) NiPbO_x and (d) NiFePbO_x . Individual elemental channels for Sn, Pb, O, and Fe were taken on the same sample spot. All samples were prepared on FTO substrate, and scale bars are 600 nm.

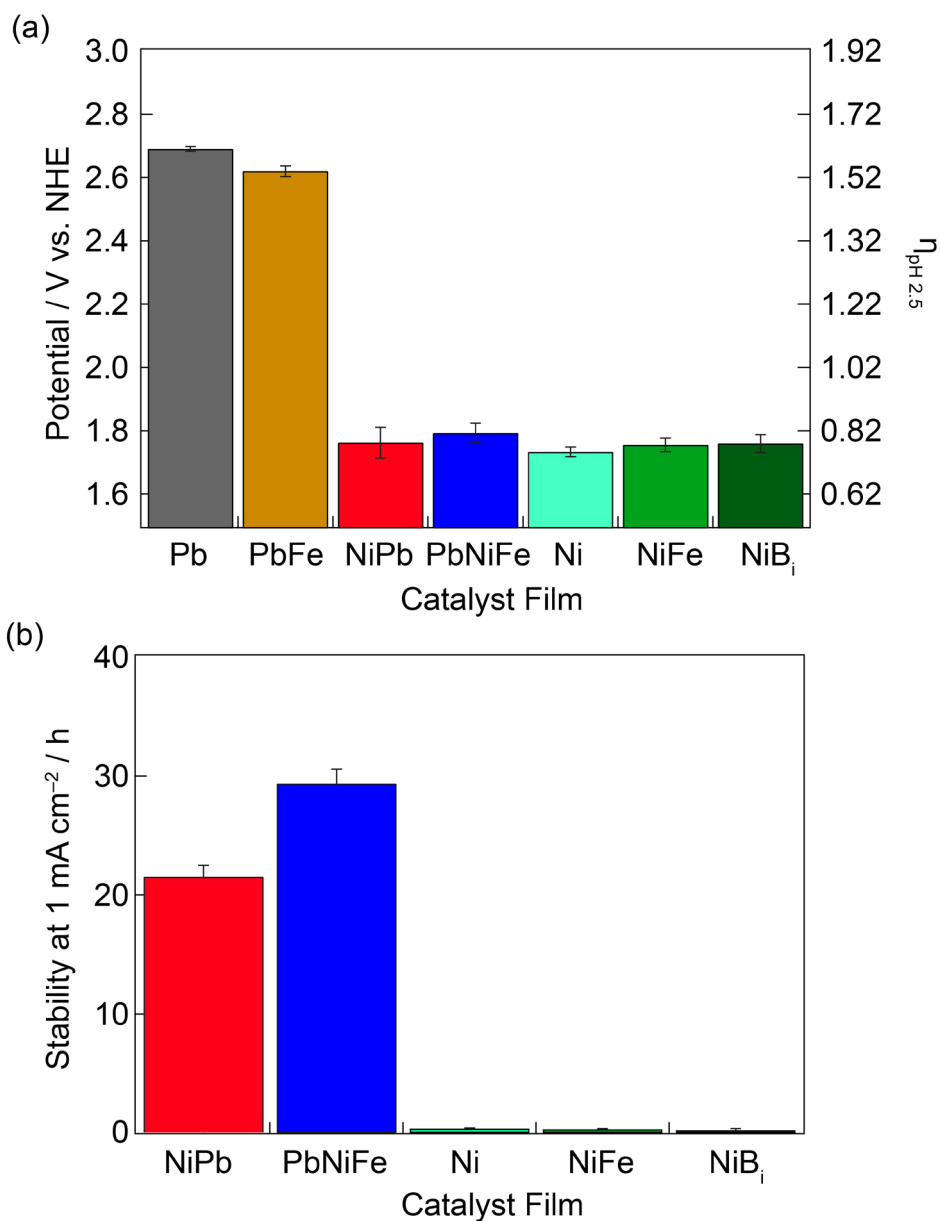


Figure S4. (a) Potential required to achieve 1 mA cm⁻² (V_{1mA}) in 0.1 M KP_i + 1.75 M KNO₃ pH 2.5 buffer for PbO_x and NiO_x based films and (b) film stability at that potential to maintain 1 mA cm⁻².

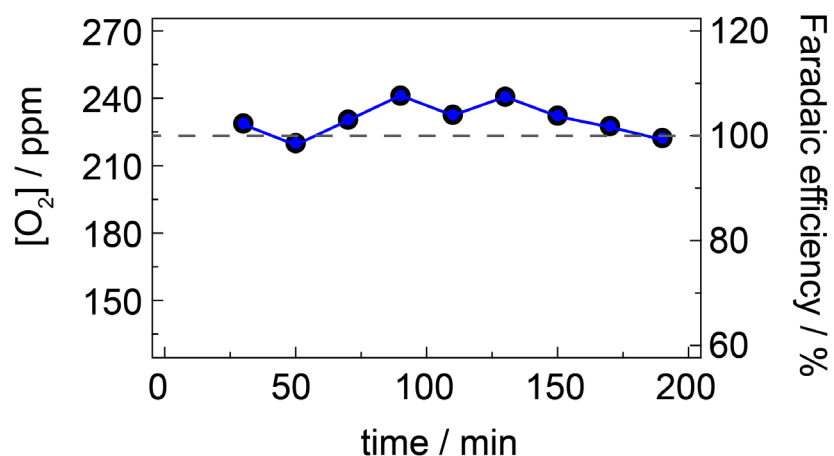


Figure S5. Measured oxygen concentration and corresponding faradaic efficiency of OER in 0.1 M KPi + 1.75 M KNO_3 pH 2.5 on NiFePbO_x film operating at 1 mA cm^{-2} (●). O_2 was detected by gas chromatography after a 30-60 min purging period. Theoretical O_2 concentrations (---) are calculated from the charge passed during chronoamperometry assuming 100% faradaic efficiency. The average faradaic efficiency is $103 \pm 3 \%$.

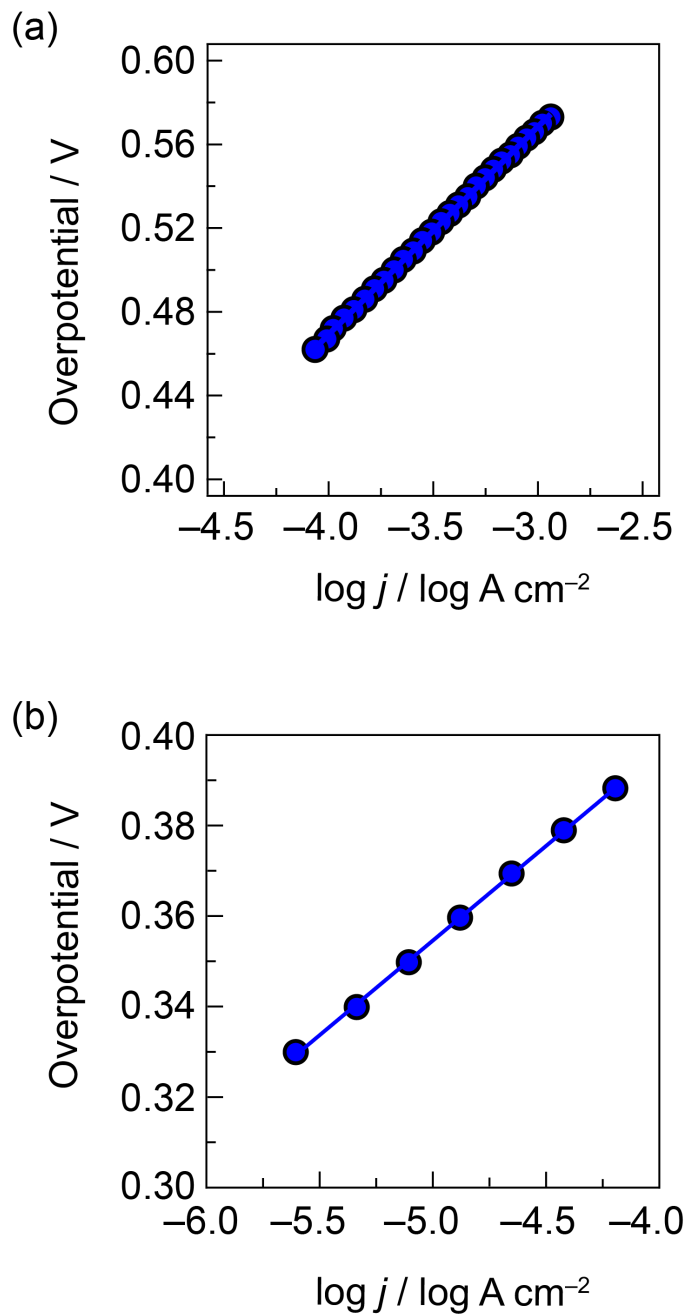


Figure S6. Representative Tafel plots of oxygen evolution for NiFePbO_x in (a) 0.1 M KPi + 1 M KNO₃ pH 7.0 and (b) 0.1 M KBi + 1 M KNO₃ pH 9.2. Tafel slope fits are 98 mV/dec and 42 mV/dec for (a) and (b), respectively.

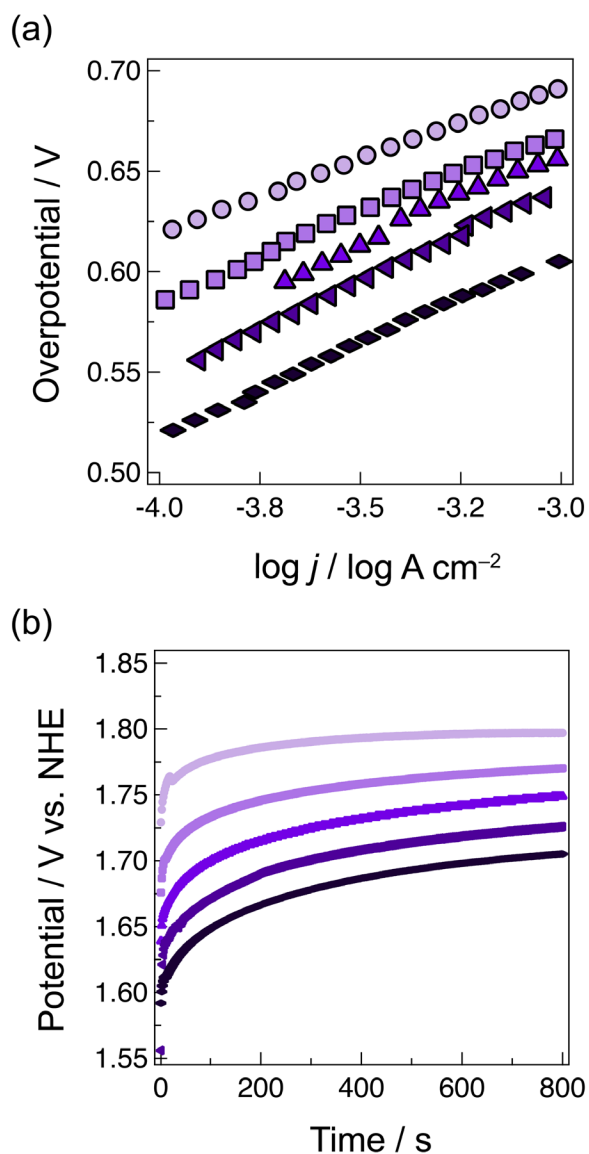


Figure S7. (a) Tafel plots of oxygen evolution for NiFePbO_x in 0.1 M KP_i + 1 M KNO₃ pH 2.5 with Ni:Fe content ratios of 1:12 (○, Tafel slope: 87.6 ± 6.1 mV/dec), 1:3 (□, Tafel slope: 96.5 ± 2.3 mV/dec), 1:1 (▲, Tafel slope: 90.1 ± 6.3 mV/dec), 3:1 (◄, Tafel slope: 88.0 ± 5.3 mV/dec), and 12:1 (◆, Tafel slope 74.2 ± 5.0 mV/dec). (b) Chronoamperometry at 1 mA cm⁻² for NiFePbO_x films in 0.1 M KP_i + 1 M KNO₃ pH 2.5 for NiFePbO_x films with Ni:Fe ratio of 1:12 (—), 1:3 (—), 1:1 (—), 3:1 (—), and 12:1 (—).

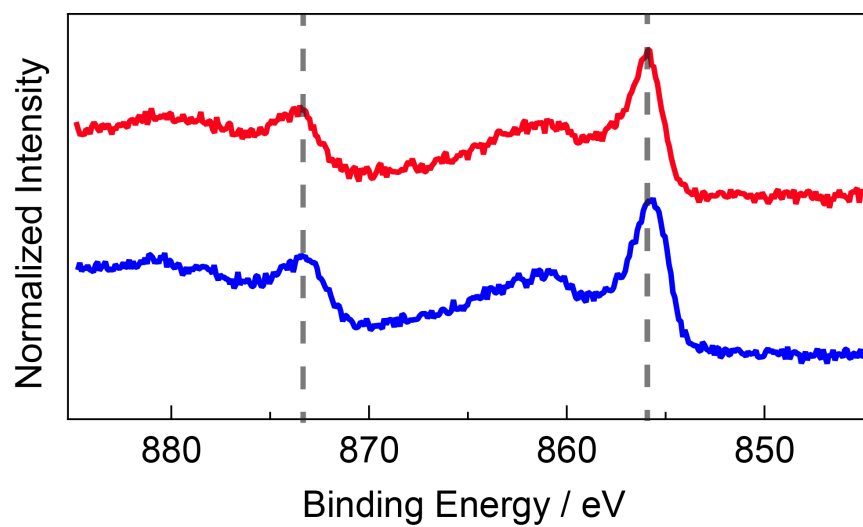


Figure S8. High-resolution XPS spectra of Ni 2*p* for NiPbO_x (—) and NiFePbO_x (—) films held at 1 mA by chronoamperometry for 10 min prior to analysis.

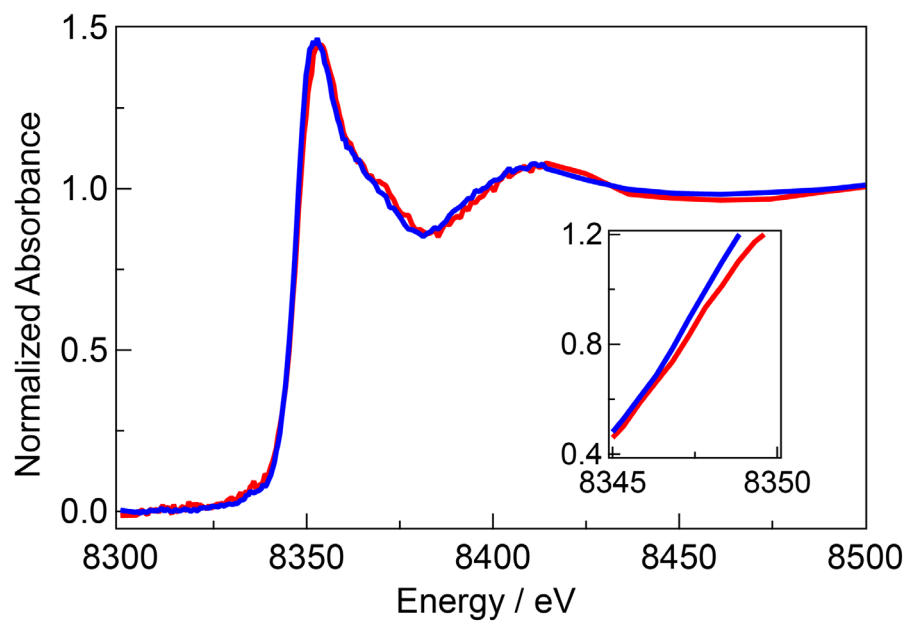


Figure S9. Ni K-edge of NiPbO_x (—) and NiFePbO_x (—) films operating OER in 0.1 M KP_i + 1 M KNO₃ pH 2.5 at 1.9 V.

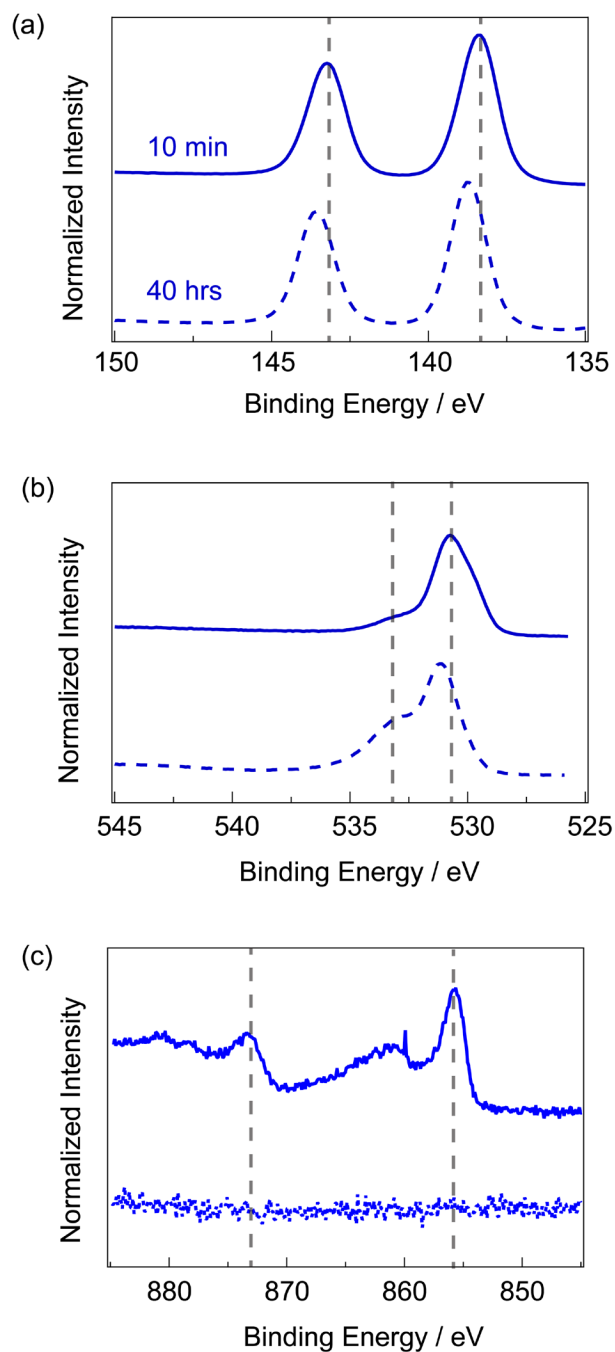


Figure S10. High-resolution XPS spectra of (a) Pb 4*f*, (b) O 1*s*, and (c) Ni 2*p* for NiFePbO_x films after maintaining an OER current of 1 mA cm⁻² for 10 min (—) and 40 h (---) in 0.1 M KPi 1M KNO₃ pH 2.5. A fresh NiFePbO_x film was prepared and conditioned (as described) for each time point analyzed.

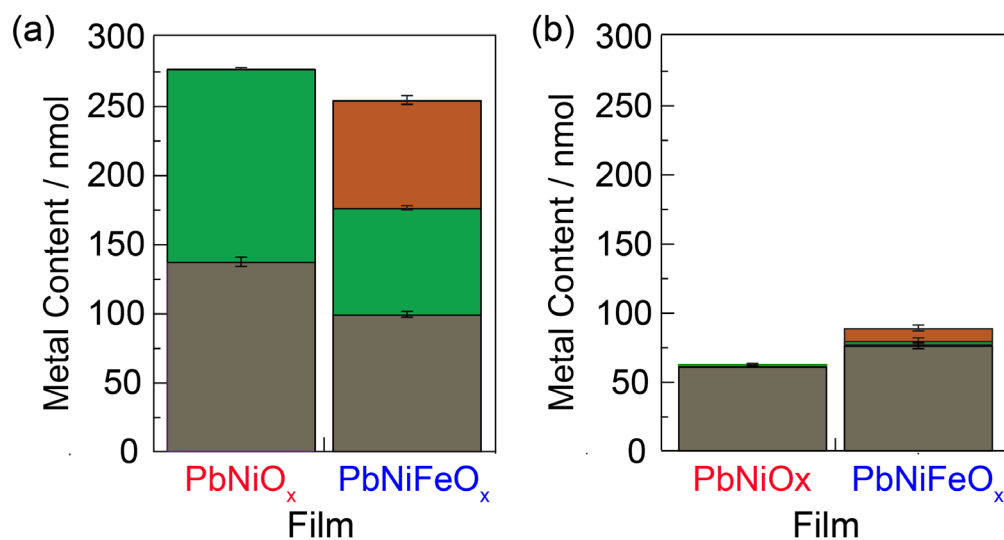


Figure S11. Metal composition: Pb (grey), Fe (brown) and Ni (green) of PbO_x based films (a) as-deposited and (b) after performing OER at 1 mA cm^{-2} in $0.1 \text{ M KP}_i + 1.75 \text{ M KNO}_3$ pH 2.5 for 40 h (this time point is well past point of film stability as indicated by large inflection in chronoamperometry curves).

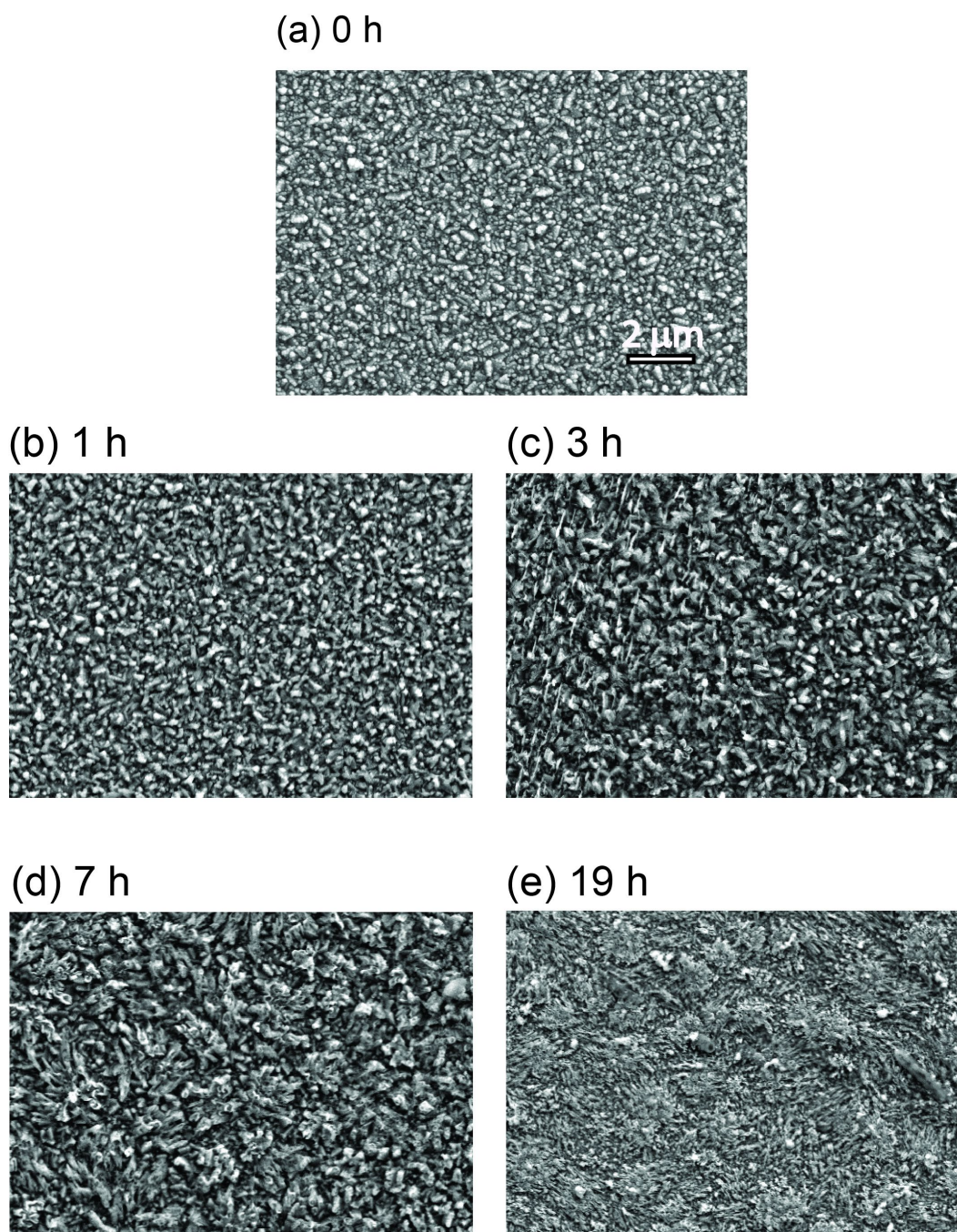


Figure S12. SEM images of NiFePbO_x film surface after performing OER at 1 mA cm⁻² in 0.1 M KP_i + 1 M KNO₃ pH 2.5 buffer for (a) 0 h, (b) 1 h, (c) 3 h, (d) 7 h, and (e) 19 h. All samples were prepared on FTO substrate, and scale bar indicates 2 μm. A fresh NiFePbO_x film was prepared and conditioned (as described) for each time point analyzed.

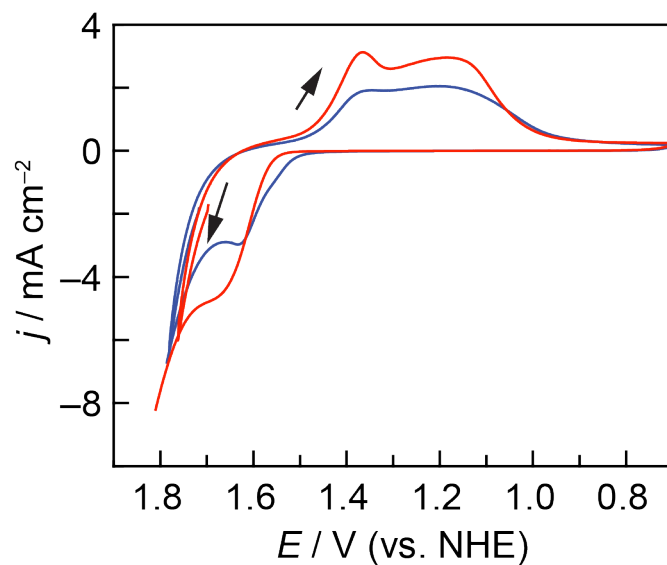
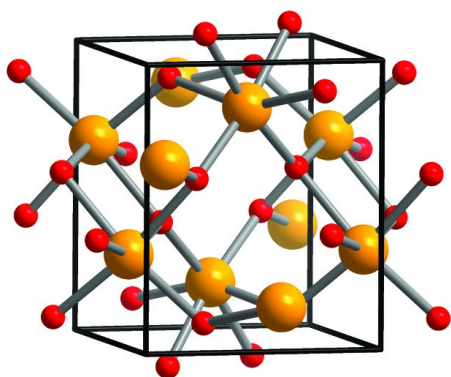


Figure S13. Cyclic voltammograms (CVs) of NiPbO_x (—) and NiFePbO_x (—) films in 1 M KNO_3 + 0.1 M KPi , pH 2.5 solution. CVs start at 1.7 V vs. NHE, and are initially scanned anodically. A scan rate of 0.1 V s^{-1} was used for both CVs.

(a)



(b)

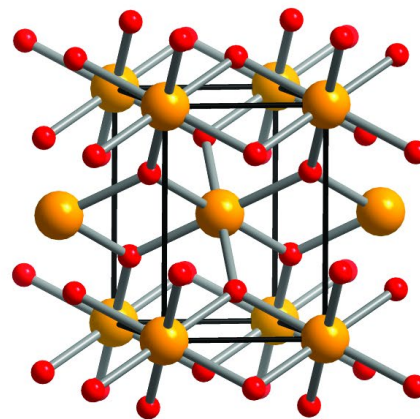


Figure S14. Structures of (a) α - PbO_2 and (b) β - PbO_2 .⁶ Pb and O atoms are colored orange and red, respectively. Black lines denote the edges of a single unit cell for each structure.

References

1. M. Huynh, T. Ozel, C. Liu, E.C. Lau, D. G. Nocera, Design of template-stabilized active and earth-abundant oxygen evolution catalysts in acid. *Chem. Sci.* **8**, 4779–4794 (2017).
2. B. Ravel, M. Newville, ATHENA, ARTEMIS, HEPHAESTUS: data analysis for x-ray absorption spectroscopy using IFEFFIT. *J. Synch. Rad.* **12**, 537–541 (2005).
3. J. F. Watts, J. Wolstenholme, An introduction to surface analysis by XPS and AES (John Wiley, 2003)
4. T. L. Barr, S. Seal, Nature of the use of adventitious carbon as a binding energy standard. *J. Vac. Sci. Technol. A* **13**, 1239–1246 (1995).
5. D. W. King, Kester, D. R. A General approach for calculating polyprotic acid speciation and buffer capacity *J. Chem. Ed.* **67**, 932–933 (1990).
6. A. Jain, S. P. Ong, G. Hautier, W. Chen, W. D. Richards, S. Dacek, S. Cholia, D. Gunter, D. Skinner, G. Ceder, K. A. Persson, Commentary: The materials project: A materials genome approach to accelerating materials innovation. *APL Mater.* **2013**, *1*, 011002.